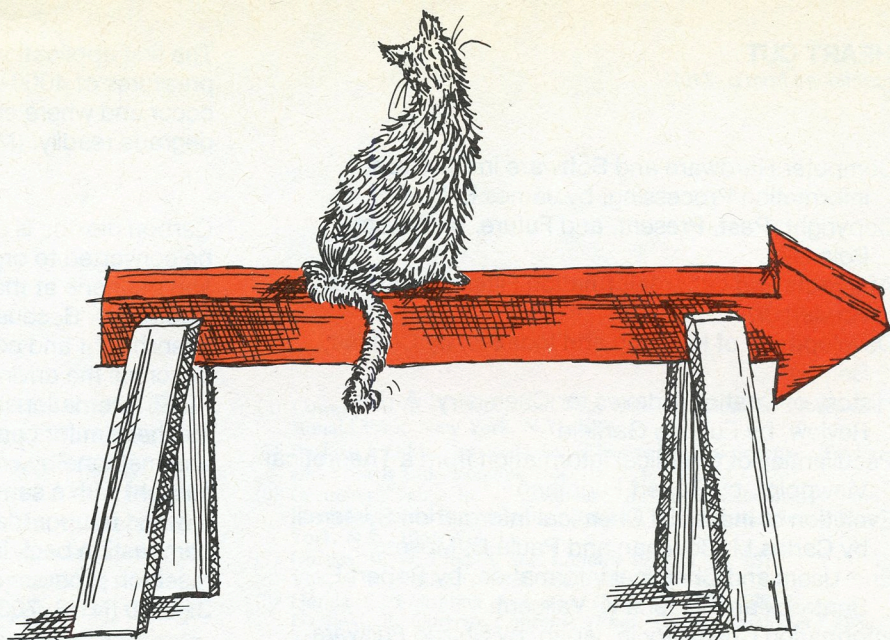# Supporting the catalyst

Israel E. Wachs
Ramzi Y. Saleh
Shirley S. Chan
Claudio Chersich

Interactions with a support can dramatically change the catalytic properties of metals or metal oxides (1, 2). For example, when V_2O_5 is supported on the anatase form of TiO_2, it is superior to unsupported V_2O_5 for catalyzing the selective oxidation of hydrocarbons (3–7). For example, vanadium pentoxide supported on TiO_2 (anatase) selectively oxidizes o-xylene to phthalic anhydride (8). Unfortunately, the mechanism by which TiO_2 modifies V_2O_5 has not been well understood (6–11). To increase our understanding of V_2O_5–TiO_2 (anatase), we decided to characterize this supported oxide system using primarily laser Raman spectroscopy (LRS), x-ray photoelectron spectroscopy (XPS), x-ray diffraction (XRD), and temperature-programmed reduction (TPR). We also observed the oxidation of o-xylene to phthalic anhydride.

TiO_2 has several structures, including anatase, rutile, brookite, and B-phase. The most common forms, rutile and anatase, are found in nature. In our investigation, we used both low- and high-surface-area anatase as support. For details concerning our materials and the experimental process, see p. 759 (Figure 1). The surface area of the low-surface-area anatase remained constant at 8–9 m^2/g upon impregnation with vanadia and subsequent calcination. X-ray diffraction detected no rutile form.

To support or not to support?

After examining the V_2O_5–TiO_2 catalyst with XRD, we applied LRS because XRD is not sufficiently sensitive to provide information about the supported vanadia. Although XRD peaks for vanadia are barely detectable for a 7% V_2O_5–TiO_2 sample, they do deviate from peaks due to bulk V_2O_5. This deviation suggests that the 100-Å V_2O_5 crystallites at the TiO_2 surface are distorted. LRS provided information about the state of supported V_2O_5 over the entire range of vanadia content. Unlike XRD, LRS detects small crystallites as well as amorphous vanadia (14, 15).

Figure 2 shows the laser Raman spectra of unsupported V_2O_5 and TiO_2 in the range ~750–1250 cm^{-1}. The bulk V_2O_5 exhibits a sharp Raman peak at 997 cm^{-1}, which is associated with the symmetrical stretching mode of the terminal double-bonded oxygen atom, V=O (16); additional bulk V_2O_5 Raman bands lie below 750 cm^{-1}.

TiO_2 has a weak second-order feature at 794 cm^{-1} in the same region; major anatase Raman bands appear at 144, 199, 399, 520, and 643 cm^{-1} (16). Strong TiO_2 Raman bands below 750 cm^{-1} complicate the detection of vanadia Raman bands in this region. Thus, we limited our present study to ~750–1250 cm^{-1}.

The laser Raman spectra of a series of V_2O_5–TiO_2 samples are shown in Figure 3. These spectra were corrected for the TiO_2 background. As the loading of V_2O_5 on TiO_2 decreases, the sharp feature associated with V_2O_5 crystallites is replaced by a broad Raman band between 850 and 1000 cm^{-1} due to a vanadia species coordinated to the TiO_2 surface (15). The broadening reflects the disordered state, or change in distribution of the density of states, of the surface vanadia species on TiO_2. The amount of vanadia required to achieve a monolayer of the surface vanadia species on the TiO_2 surface may be estimated from the area occupied per $VO_{2.5}$ unit of bulk V_2O_5, which is 0.105 nm^2; this corresponds to about 1.3% V_2O_5–TiO_2 (17). The lowest loading of vanadia that exhibits the crystalline V_2O_5 Raman feature at 997 cm^{-1} is 2% V_2O_5–TiO_2. Thus, it appears that approximately a monolayer of the surface vanadia species forms on the TiO_2 surface prior to the formation of V_2O_5 crystallites. At V_2O_5 loadings exceeding 1.9% V_2O_5–TiO_2, small crystallites of V_2O_5 are present on the anatase support in addition to the monolayer of the surface vanadia. Thus, two states of vanadia exist in V_2O_5–TiO_2 samples calcined at 450 °C.

A broad band between 850 and 1000 cm^{-1} dominates the laser Raman spectra of the high-surface-area V_2O_5–TiO_2 samples (Figure 4). Comparison of 3% V_2O_5–TiO_2 samples from Figure 3 and Figure 4 shows that the state of vanadia also depends on the surface area of TiO_2. High-surface-area anatase accommodates an order of magnitude more surface vanadia than low-surface-area anatase before a vanadia monolayer is achieved. Thus, the relative amounts of the surface and crystalline V_2O_5 depend on the surface area of the support and the content of vanadia. All subsequent data will be limited to low-surface-area V_2O_5–TiO_2 samples.

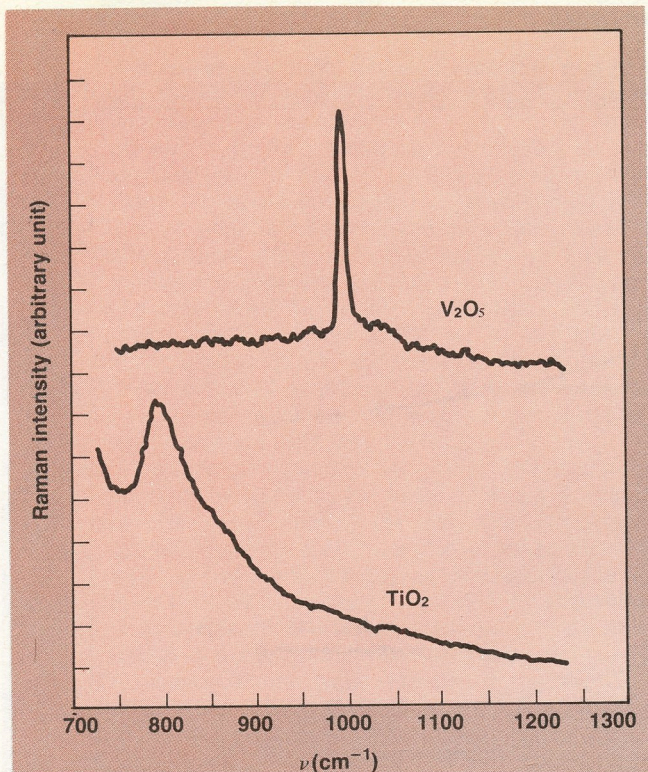The Raman intensities of the surface vanadia species in Figure 3, i.e., 0.7% vs 1.4%, are not proportional to the

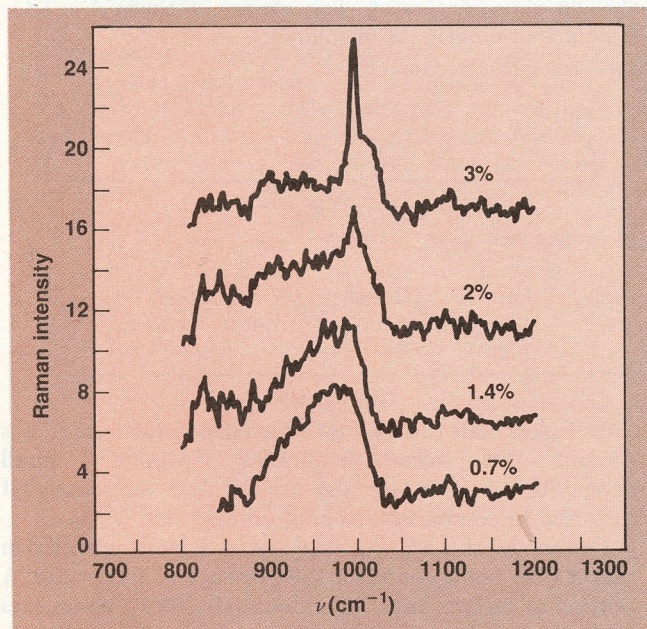**Figure 2.** Laser Raman spectra of unsupported V_2O_5 and TiO_2

Figure 3. Laser Raman spectra of low-surface-area V_2O_5–TiO_2. (All spectra corrected for TiO_2 background)

vanadia content because of the increase in the sample color with increasing vanadia content. The white TiO_2 support became strongly colored with increasing vanadia content, which increased the optical absorbence of the samples. This is apparent from the strong suppression of the anatase Raman bands. It suggests that as the vanadia content increases, the Raman scattering occurs from a progressively thinner layer located near the front surface of the sample.

X-ray photoelectron spectroscopy revealed that the supported vanadia is present as V^{5+}. The XPS V $2p_{3/2}$
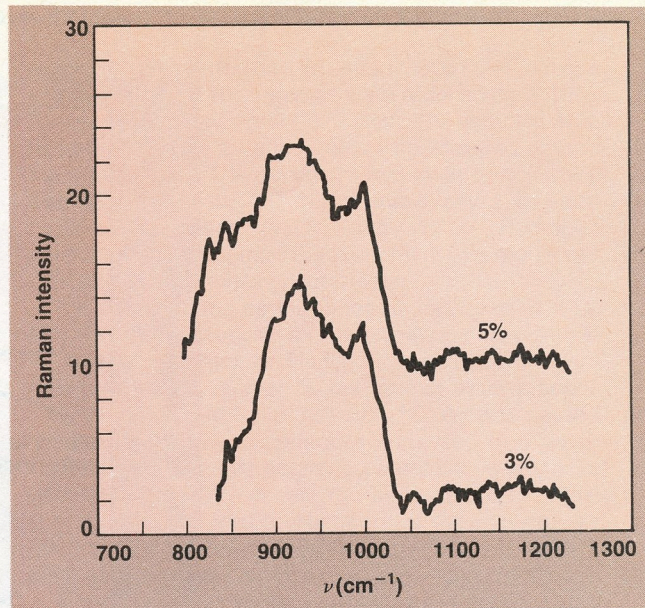

Figure 4. Laser Raman spectra of high-surface-area V_2O_5–TiO_2. (All spectra corrected for TiO_2 background)

Table 1. Binding energies of V_2O_5–TiO_2 samples (using XPS)

Sample	Binding energies (eV)	
	V $2p_{3/2}$	O 1s
1.4% V_2O_5–TiO_2^a	517.4	529.8
7.0% V_2O_5–TiO_2^a	517.3	529.9
$V_2O_5^b$	517.4	530.2

[a] Referenced to Ti $2p_{3/2}$ at 458.5 eV.
[b] Referenced to C 1s at 284.6 eV.

binding energies of V_2O_5–TiO_2 samples, presented in Table 1, are independent of vanadia content. This observation agrees with recent electron spin resonance (ESR) studies concluding that the amount of V^{4+} in V_2O_5–TiO_2 catalysts calcined at 500 °C is negligible (11). In situ XPS reduction experiments with H_2 at 450 °C demonstrated that supported V^{5+} readily reduces to V^{3+}, which has a binding energy of 515.6 eV (18). We also examined the reduction behavior of the V_2O_5–TiO_2 samples and unsupported V_2O_5 with TPR. Vanadia supported on titania reduced more readily than did unsupported V_2O_5.

Catalytic performance

The o-xylene oxidation reaction is complex and yields many different products (Figure 5). We maintained the reaction temperature above 320 °C to prevent formation of tarlike reaction products, which occur at lower temperatures and conversions and can plug the gas chromatograph valves (7). Phthalic anhydride was the major C_8–oxygenate product; toluraldehyde and phthalide accounted for only a few percent of the reaction products. Maleic anhydride was the only oxygenate by-product formed at high conversions, and it most probably originated from the complete oxidation of phthalic anhydride.

We examined the catalytic performance of unsupported V_2O_5 and V_2O_5–TiO_2 for o-xylene oxidation. The reactivity, reflected in the temperature required to achieve 60% conversion and selectivity of V_2O_5–TiO_2
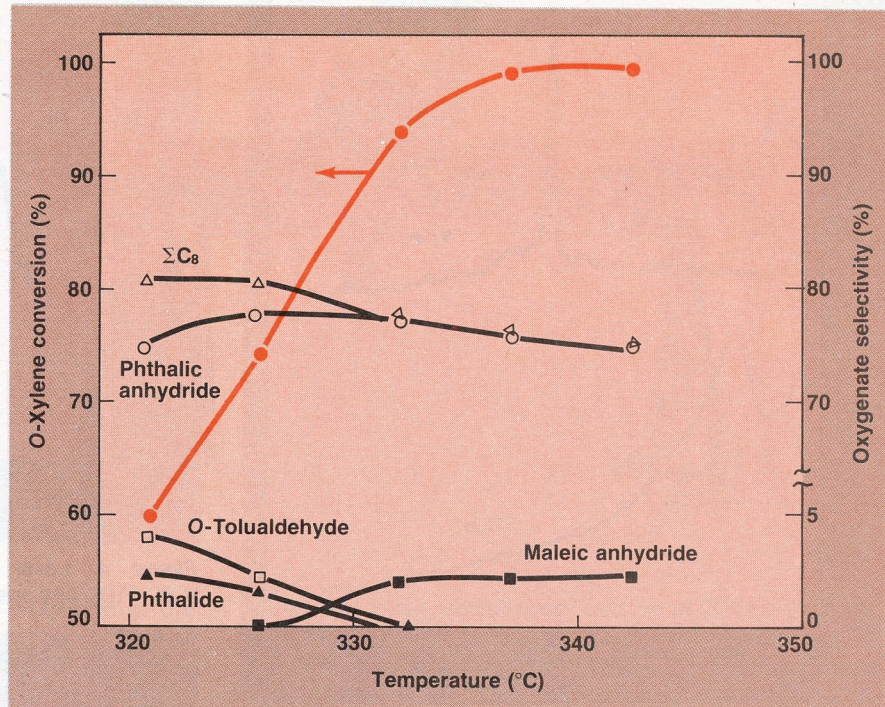
Figure 5. Conversion of *o*-xylene and selectivity toward various oxidation products for 7% V_2O_5–TiO_2 sample

catalysts toward *o*-xylene oxidation, is illustrated in Figure 6. With less than monolayer coverage of the surface vanadia species, < 1.9% V_2O_5–TiO_2, activity and selectivity increase markedly with increasing vanadia content. With more than a monolayer of vanadia, 1.9–7.0% V_2O_5–TiO_2, activity and selectivity of this reaction are not influenced by the vanadia content. However, as the vanadia content is increased to 21%, the activity and selectivity decrease. Unsupported V_2O_5 catalyst displays low activity and selectivity. (We corrected the conversion data for the lower surface area of the unsupported V_2O_5 catalyst, 4–5 m^2/g, relative to the V_2O_5–TiO_2 catalysts so that all catalysts were compared on a similar surface area basis.)

The LRS data reveal two states of vanadia present in V_2O_5–TiO_2 catalysts: a surface vanadia species and crystalline V_2O_5. Furthermore, the formation of surface vanadia precedes the formation of crystalline V_2O_5, which appears only after a monolayer of surface vanadia covers the TiO_2 surface. The preferred formation of the vanadia monolayer reflects the strong interaction between vanadia and TiO_2. However, different preparation techniques may yield some crystalline V_2O_5 prior to the completion of the monolayer. The interaction of vanadia with TiO_2 contrasts sharply with the interaction of vanadia and SiO_2. For V_2O_5–SiO_2, crystalline V_2O_5 is present at extremely low coverages of vanadia and reflects weak interaction between vanadia and the SiO_2 surface (*15*). The surface vanadia species coordinated to TiO_2 are present in the 5+ oxidation state. However, the coordination of the surface vanadia species cannot be assigned from the LRS data. Recent extended x-ray absorption fine structure (EXAFS) and x-ray absorption near edge structure (XANES) measurements by Kozlowski et al. suggest that the surface vanadium oxide has two terminal bonds (1.65 ± 0.05 Å) and two bridging bonds (1.90 ± 0.5 Å) to oxygen and exhibits intrinsic disorder (*10*). Additional studies,

however, are necessary to confirm the structure of the surface vanadia species. The model of the V_2O_5–TiO_2 system that emerges is as follows:

Less than monolayer coverage:
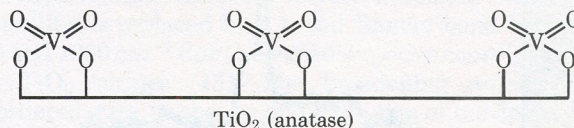
More than monolayer coverage:
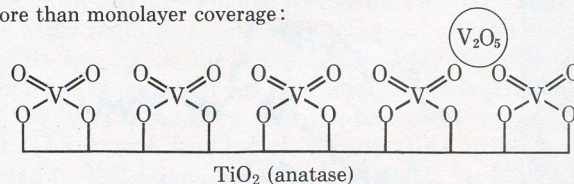
With less than 1.9% V_2O_5–TiO_2, only surface vanadia is present. With more than 1.9% V_2O_5–TiO_2, small crystallites of V_2O_5 are also present and are somewhat distorted in comparison to bulk unsupported V_2O_5.

Our model of the V_2O_5–TiO_2 system is oversimplified in that it does not account for the presence of impurities. A portion of surface vanadia undoubtedly forms complexes with some of the surface impurities present on the titania support. This may account for the observation that the amount of vanadia required to achieve a monolayer on low-surface-area TiO_2 was somewhat greater than that estimated from geometric considerations, that is, 1.9% vs. 1.3% V_2O_5.

Vanadia supported on other oxides

Both states of vanadia in V_2O_5–TiO_2 reduce more readily than unsupported V_2O_5. Roozeboom et al. made similar observations for vanadia supported on other oxides, including Al_2O_3 and SiO_2 (*15*). The enhanced reduction of the small V_2O_5 crystallites bears out with reduction studies of V_2O_5 crystals in an optical microscope (*19*), which found that the rate of reduction increased with decreasing

For our investigation, we used both low- and high-surface-area TiO_2 (anatase) as supports. We obtained low-surface-area anatase, 8–9 m^2/g, from Mobay Corporation. By hydrolyzing titanium isopropoxide and then calcining it at 550 °C for 2 h we prepared high-surface-area anatase with a surface area of ~80 m^2/g. Our study deals primarily with the low-surface-area TiO_2 with only brief reference to the high-surface-area TiO_2 support. The impurities present in the TiO_2 supports were determined by atomic absorption. The high-surface-area TiO_2 contained 0.21 wt % Al, 0.24 wt % Sn, and 0.08 wt % Ca. The Mobay anatase contained 0.15 wt % K, 0.10 wt % P, 0.10 wt % Al, and 0.16 wt % Si. XPS measurements confirmed the presence of K and P on the surface of Mobay anatase.

X-ray diffraction patterns were obtained with a Philips diffractometer using Cu $K\alpha$ radiation and a diffracted-beam monochromator. X-ray diffraction examination confirmed that both the high- and low-surface-area TiO_2 contained only the anatase phase; the rutile phase was absent in the XRD patterns.

We prepared $V_2–TiO_2$ catalysts by dissolving V_2O_5 in aqueous oxalic acid and impregnating the TiO_2 support. Excess water was allowed to evaporate at ~65 °C. The catalysts were subsequently dried at 110 °C and calcined in oxygen at 450 °C for 2 h. The V_2O_5 in the samples varied from 0.7 to 21.0 wt % V_2O_5. We obtained unsupported V_2O_5 with a surface area of 4–5 m^2/g from Alfa Corporation.

X-ray photoelectron spectroscopy measurements were made with a Leybold–Heraeus LHS-10 electron spectrometer. The x-ray was generated by an aluminum anode operated at 12 kV and 25 mA, and the Ti $2p_{3/2}$ peak at 458.5 eV served as a reference for the binding energies of the V $2p_{3/2}$ signals (12). We also performed in situ XPS measurements with this unit (13).

In Reference 13 we describe the multichannel laser Raman spectrometer in detail. For the excitation we tuned an argon ion laser (Spectra Physics, Model 165) to the 514.5-nm line. The laser power at the sample location was set at 40 mW. The Raman spectrometer, a triple monochromator (Model DL203 from Instruments SA), was coupled to an optical multichannel analyzer from Princeton Applied Research (Model OMA2). This analyzer can deliver a spectrum about 100 times faster than a conventional scanning spectrometer and also permits measurements on samples with weak signals. The overall resolution was about 6 cm^{-1}.

We determined the reducibility of the vanadia catalysts by applying TPR; 10–100 mg of sample was supported on a fritted disk in a quartz tube (¼-in. outside diameter [o.d.]). The samples were reduced by a 10 % H_2–He mixture flowing at 50 cc/min. The samples were heated at 1 °C/s by a nichrome wire wrapped around the quartz tube. The maximum reduction temperature was maintained at 700 °C to avoid any solid-state reactions between V_2O_5 and TiO_2. Hydrogen consumption during the TPR experiment was monitored with a UTI-100C mass spectrometer.

We examined the performance of unsupported V_2O_5 and $V_2O_5–TiO_2$ catalysts for the oxidation of o-xylene in the reactor unit illustrated in Figure 1. All catalysts were examined with 1.25 mol % o-xylene in air at a space velocity of 2760 h^{-1} and 320–380 °C. Air was passed through the o-xylene generator immersed in a water bath. Thermostatically controlled water circulated to the generator bath to maintain the temperature to within 0.1 °C. We analyzed a slipstream of the o-xylene–air feed for all gases and organic components with a calibrated on-line multicolumn gas chromatograph equipped with a thermal conductivity detector. After establishing the desired o-xylene concentration, we diverted the feed to the reactor immersed in a molten salt bath. The temperature of the salt bath was maintained to within 1°C.

A slipstream of the reactor effluent was analyzed by the gas chromatograph for o-xylene conversions and reaction products. The main reaction products observed were phthalic anhydride, tolualdehyde, phthalide, maleic anhydride, CO, CO_2, and water. We ignored other products, including citraconic acid and benzoic acid, because they were present in small quantities. At each temperature the reactor effluent was analyzed three to five times; this was followed by several feed analyses. The carbon balance was always within 5 %. The reactor was usually blanketed with N_2 during start-up and overnight while the feed was being analyzed. The reactor, 0.5-in.-o.d., 316 stainless steel, was fitted with a thermocouple to monitor the temperature throughout the catalyst bed. The feed, which was preheated to the salt bath temperature, entered the reactor from the bottom. We packed the reactor with 2 cc of catalyst and 1.92 g of $V_2O_5–TiO_2$ with particle diameters of 0.4–0.7 mm, diluted with 8 cc of 0.5-mm glass beads. This catalyst dilution ratio gave an isothermal profile along the length of the catalyst bed. The remaining reactor volume was filled with 3-mm glass beads, 2 cc at the top and bottom. Blank runs showed the reactor walls and beads to be inert to o-xylene oxidation at the temperature range we investigated.
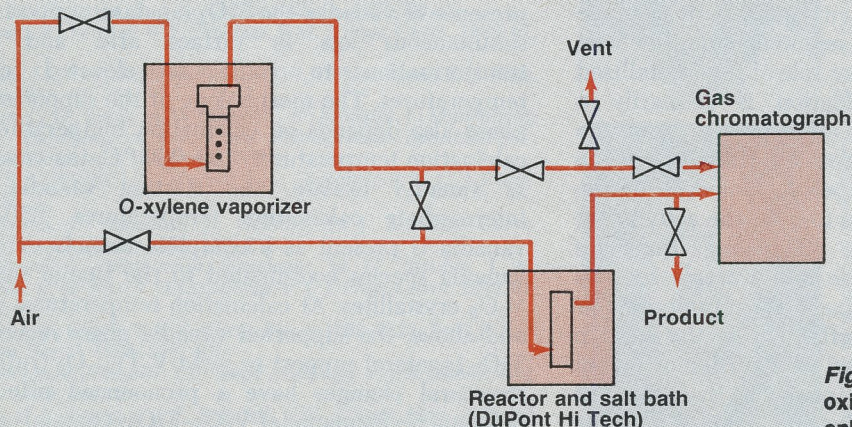

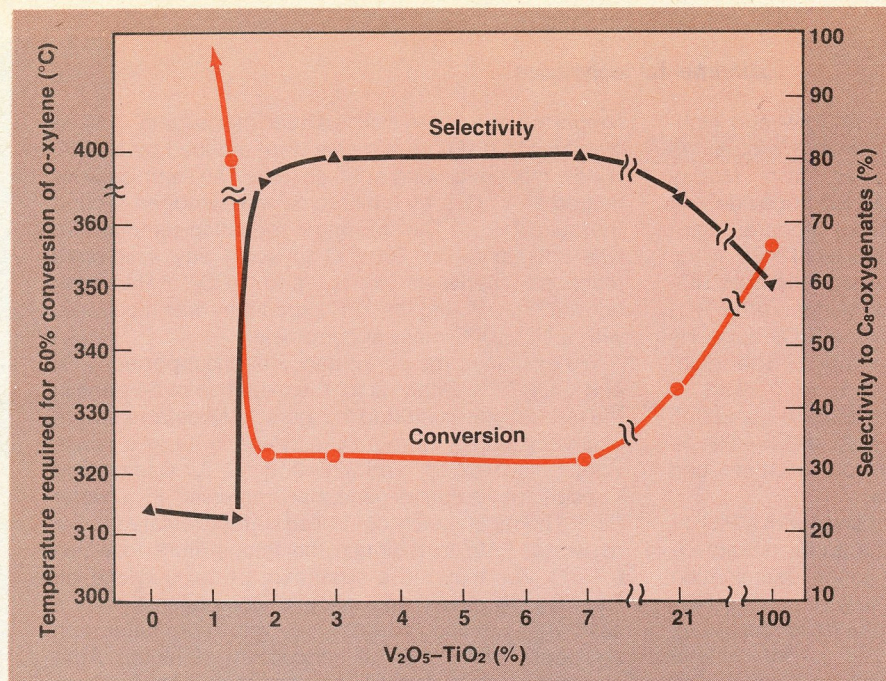**Figure 1.** Reactor for the oxidation of o-xylene to phthalic anhydride

Figure 6. o-Xylene activity and selectivity toward C₈–oxygenates over unsupported V₂O₅ and V₂O₅–TiO₂ catalysts

thickness of the V_2O_5 crystal in the c direction. Apparently, crystallite dimensions affect the reducibility of crystalline V_2O_5. The enhanced reduction kinetics of the surface vanadia species must be related to the vanadia–support interaction. However, this is not unique to TiO_2; Roozeboom et al. found the same behavior on other oxide supports (15).

Until a monolayer forms, oxidation activity depends strongly on the amount of vanadia coverage on the support, because TiO_2 is essentially inactive for the oxidation of o-xylene (Figure 6). Selectivity with less than a monolayer of coverage of vanadia, however, is extremely low. Exposed titania sites may lead to complete combustion of C_8–oxygenates. We confirmed this when we mixed TiO_2 with an active and selective V_2O_5–TiO_2 catalyst and obtained lower product selectivity. Thus, TiO_2 must be covered by a *complete* monolayer of the surface vanadia species to be an active and selective catalyst for the oxidation of o-xylene to phthalic anhydride. Gellings et al. reached similar conclusions during their investigation of toluene oxidation over V_2O_5–TiO_2 catalysts (50 m²/g; 65% anatase; 35% rutile) (20). Bond et al. demonstrated that a V_2O_5–TiO_2 catalyst containing a monolayer of vanadia is active and selective for the oxidation of o-xylene to phthalic anhydride (7).

With more than monolayer coverage of vanadia, from 1.9% to 7.0% V_2O_5–TiO_2, the activity and selectivity of the o-xylene oxidation reaction are essentially uninfluenced by the vanadia content. The minor role of the crystallized V_2O_5 phase for o-xylene oxidation is primarily a consequence of the low effective surface area of the crystals relative to the higher effective surface area of the monolayer of surface vanadia species. However, as the vanadia content further increases to 21%, the activity for o-xylene oxidation diminishes, suggesting that the supported crystalline V_2O_5 phase is not active for this oxidation reaction. Thus, crystalline V_2O_5, unsupported or supported on TiO_2, is not as effective as the surface vanadia species. Gasior and Machej recently demonstrated that the crystallographic plane of V_2O_5 that contains exposed V=O bonds is more active and selective than the other V_2O_5 planes for the oxidation of o-xylene to phthalic

anhydride (21). The maximum selectivity for phthalic anhydride over the unsupported V_2O_5 catalysts is inferior to that obtained with active V_2O_5–TiO_2 catalysts.

The V_2O_5–TiO_2 (anatase) catalysts removed from the o-xylene oxidation reactor were also characterized after exposure to air (23). Analysis of the spent catalysts showed that the V_2O_5 crystallites originally present in the fresh catalysts were partially reduced by the o-xylene reaction environment to lower oxides of crystalline vanadium oxide. The surface vanadia species coordinated to the TiO_2 (anatase) support, however, were found to be fully oxidized in the spent catalysts. The surface vanadia was most probably also partially reduced in the o-xylene reaction environment but was reoxidized by the ambient environment prior to the characterization. The more facile oxidation of the surface vanadia is probably related to the fact that, unlike the crystalline vanadia phase, every surface vanadia species is exposed to the environment. The analysis of the spent V_2O_5–TiO_2 (anatase) catalysts further confirmed that the monolayer of surface vanadia species and crystalline vanadia phases remains intact during the o-xylene oxidation reaction.

The interaction of V_2O_5 with the surface of TiO_2 (anatase) was also studied over the temperature range 110–750 °C (24, 25). The state of V_2O_5–TiO_2 (anatase) is strongly dependent on calcination temperature. In the presence of vanadia, the TiO_2 (anatase) support exhibits a simultaneous loss in surface area and structural transformation to rutile at elevated calcination temperatures. The morphology of the supported vanadia phase also depends on calcination temperature. At low calcination temperatures, 100–200 °C, the vanadia exists as vanadyl oxalate, the starting vanadia salt. At intermediate calcination temperatures, 350–575 °C, vanadia is present as a complete monolayer of surface vanadia species coordinated to the titania support and V_2O_5 crystallites. At calcination temperatures of 575 °C and above, the supported vanadia phase reacts with the TiO_2 (anatase) support to yield $V_xTi_{1-x}O_2$ (rutile). These structural changes have a pronounced effect on the catalytic performance of V_2O_5–TiO_2 (anatase) catalysts for the oxidation of o-xylene. The optimum catalytic

performance is observed for prolonged calcination at intermediate temperatures, 350–575 °C, where a complete monolayer of surface vanadia exists on the TiO_2 (anatase) support.

Our study demonstrates that vanadia coordinated to the TiO_2 support is the active site in V_2O_5–TiO_2 catalysts for o-xylene oxidation to phthalic anhydride. Moderate amounts of crystalline V_2O_5 do not affect the catalytic performance of V_2O_5–TiO_2 catalysts for o-xylene oxidation because of the low effective surface area and poor catalytic activity of this crystallized phase. Van Hengstum et al. similarly demonstrated that moderate amounts of crystalline V_2O_5 do not affect the oxidation of toluene over V_2O_5–TiO_2 catalysts (20). Furthermore, Bond et al. suggested that the nature of the surface vanadia species on the TiO_2 support depends on the catalyst preparation method (7). Our work and that of Roozeboom et al. and Van Hengstum using different preparation techniques has shown that the properties of the surface vanadia species are independent of the preparation method but are intrinsic to the vanadia–titania interaction (15, 20, 22).

Acknowledgment

References

(1) Tauster, S. J.; Fung, S. C.; Baker, R.T.K.; Horsley, J. A. *Science* **1981**, *211*, 1121.
(2) Soled, S.; Murrell, L.; Wachs, I.; McVicker, G. In "Solid State Chemistry in Catalysis"; ACS Symposium Series No. 279; American Chemical Society: Washington, D.C., 1985, p. 165.
(3) Vanhove, D.; Blanchard, M. *Bull. Sci. Chim. Fr.* **1971**, 3291.
(4) Grabowski, R.; Grzybowska, B.; Haber, J.; Sloczynski, J. *React. Kinet. Catal. Lett.* **1975**, *2*, 81.
(5) Bond, G. C.; Sarkany, J.; Parfitt, G. D. *J. Catal.* **1979**, *57*, 476.
(6) Murakami, Y.; Inomata, M.; Miyamoto, A.; Mori, K. In "Proceedings of the 7th International Congress on Catalysis, Tokyo," Elsevier: Amsterdam, the Netherlands, 1981; p. 1344.
(7) Bond, G. C.; Konig, P. *J. Catal.* **1982**, 77, 309; Bond, G. C.; Bruckman, K. *Faraday Discuss. Chem. Soc.* **1981**, 72, 235.
(8) Wainwright, M. S.; Foster, N. R. *Catal. Rev.—Sci. Eng.* **1979**, *19*, 211.
(9) Vejux, A.; Courtine, P. *J. Solid State Chem.* **1978**, *23*, 93.
(10) Kozlowki, R.; Pettifer, R. F.; Thomas, J. M. *J. Phys. Chem.* **1983**, 87, 5176.
(11) Inomata, M.; Mori, K.; Miyamoto, A.; Ul, T.; Murakami, Y. *J. Phys. Chem.* **1983**, 87, 754.
(12) Wagner, C. D.; Riggs, M. W.; Davis, L. E.; Moulder, J.; Muilenberg, G. E. "Handbook of X-Ray and Photoelectron Spectroscopy"; Physical Electronics Industries, 1979.
(13) Chan, S. S.; Wachs, I. E.; Murrell, L. L.; Dispenziere, N. C. *J. Catal.* **1985**, *92*, 1.
(14) Roozeboom, F.; Medema, J.; Gellings, P. J. *Z. Phys. Chem. (Frankfurt am Main)* **1978**, *111*, 215.
(15) Roozeboom, F.; Mittelmaijer-Hazeleger, M. C.; Moulijn, J. A.; Medema, J.; de Beer, V.H.J.; Gellings, P. J. *J. Phys. Chem.* **1980**, *84*, 2783.
(16) Beattie, I. R.; Gilson, T. R. *J. Chem. Soc. A* **1969**, 2322; *Proc. R. Soc. London, Ser. A* **1968**, *307*, 407.
(17) Roozeboom, F.; Fransen, T.; Mars, P.; Gellings, P. J. *Z. Anorg. Allg. Chem.* **1979**, *449*, 25.
(18) Colton, R. J.; Guzman, R. J.; Rabalais, J. W. *J. Appl. Phys.* **1978**, *49*, 409.
(19) Tilley, R.J.D.; Hyde, B. G. *J. Phys. Chem. Solids* **1970**, *31*, 1613.
(20) Van Hengstum, A. J.; Van Ommen, J. G.; Bosch, H.; Gellings, P. J. *Appl. Catal.* **1983**, 8, 369.
(21) Gasior, M.; Machej, T. *J. Catal.* **1983**, *83*, 472.
(22) Van Hengstum, A. J.; Van Ommen, J. G.; Bosch, H.; Gellings, P. J. *Appl. Catal.* **1983**, 5, 207.
(23) Wachs, I. E.; Chan, S. S.; Saleh, R. Y. *J. Catal.* **1985**, *91*, 366.
(24) Wachs, I. E.; Chan, S. S.; Chersich, C. C. In "Reactivity of Solids"; Barret, P.; Dufour, L. C., Eds.; 1985; p. 1047.
(25) Saleh, R. Y.; Wachs, I. E.; Chan, S. S.; Chersich, C. C. *J. Catal.*, in press.
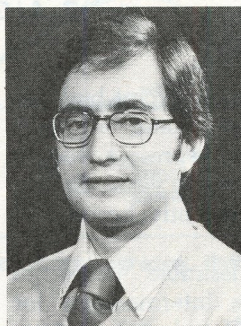
Israel E. Wachs received his chemical engineering degrees from the City College of the City University of New York (B.E.) and Stanford University (M.S. and Ph.D.). He has been employed by the Corporate Research Science Laboratories of Exxon Research and Engineering Company (Clinton Township, Route 22 East, Annandale, N.J. 08801) since graduating from Stanford. He has been involved in fundamental and applied research of heterogeneous catalysis.

Ramzi Y. Saleh received his M.S. in physical chemistry from Carnegie–Mellon University and his Ph.D. in physical chemistry from the University of Pittsburgh. He subsequently joined Norton Company, where he became involved in many different areas of heterogeneous catalysis. He started work with Exxon Chemicals, Intermediates Technology Division (Baton Rouge, La. 70821) in 1980. He has concentrated on phthalic anhydrides.

Shirley Suiling Chan received her M.S. in physics and Ph.D. in biophysics from the University of Illinois, Urbana. In both her graduate research and postdoctoral research at the Max Planck Institute for Biophysical Chemistry, West Germany, she applied laser technologies to the studies of protein and cell dynamics. She is a senior scientist at the Technical Center of the British Oxygen Corporation Group (Murray Hill, N.J. 07974) engaged in research and development of health care instruments.
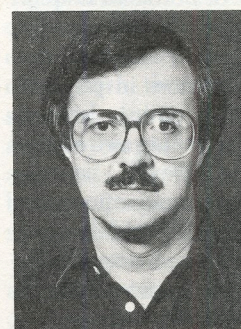
Claudio C. Chersich graduated from the Bernini Institute in Rome, Italy. After graduation he became involved in the technical applications of diamond drill bits at Christensen Diamond Products Company. He subsequently joined Halcon, working in R&D on oxidation catalysts. He was hired by Exxon Research and Engineering Company in 1979 and has been involved in fundamental and applied research of heterogeneous catalysts. He is now with Exxon Chemical Elastomers Division (Linden, N.J. 07036).